for $n > 1$ do not conform with expectations and the direction of changes observed in the case of complex **1**: $[Fe(H_2O)_5X]^{2+}$ (X = carbamide derivative). However, they are closely associated with the changes in adsorption of carbamide derivatives, and their analysis allows us to conclude that the strong adsorption of carbamide derivatives brings about the increase in the stability of complexes due to the formation of complexes with the participation of adsorbed ligand: $[Fe(H_2O)_{5-n}X_n(X)_{ads}]^{2+}$.

Contribution from the Department of Chemistry,
University of Houston—University Park, Houston, Texas 77004

Electrochemical and Spectroelectrochemical Studies of Monomeric Rhodium(III) Porphyrins in Nonaqueous Media

K. M. Kadish,* C.-L. Yao, J. E. Anderson, and P. Cocolios†

Received July 13, 1984

The electrochemistry and spectroelectrochemistry of (TPP)Rh(NH(CH$_3$)$_2$)Cl and (TPP)Rh(NH(CH$_3$)$_2$)$_2^+$Cl$^-$ were investigated in benzonitrile, THF, and pyridine. In benzonitrile, both of these six-coordinated Rh(III) complexes undergo two reductions and two oxidations at room temperature. No oxidations are observed in THF or pyridine (due to the limited solvent window), but two reductions are observed for the two complexes in each of these solvents. The first reduction is followed by a rapid chemical reaction, which generates a diamagnetic species that appears to be a rhodium(II) dimer. The second reduction is a two-electron reaction that produces another diamagnetic species. Electronic absorption spectra indicate the second reduction is at the porphyrin π system. The two oxidations generate the cation radical and dication of the Rh(III) compounds and give electronic absorption and ESR spectra similar to those of other metalloporphyrin π radical cations and dications. On the basis of the electrochemical and spectroscopic results, an overall oxidation–reduction scheme was formulated.

Introduction

Numerous communications have appeared in the literature that report the synthesis of rhodium(III) and rhodium(II) porphyrins,[1-14] but very little is known about the electrochemistry of these complexes. No electrochemical data has ever been reported for the reduction of rhodium(III) or rhodium(II) porphyrins, and only a single paper has been published that reports electrooxidation of rhodium(III) porphyrins.[15] One of the few examples of a monomeric rhodium(II) porphyrin species, identified by ESR and elelctronic absorption spectra, was reported in a recent paper.[16] The four-coordinate (TPP)Rh^{II} was generated by flash photolysis in 2-methyltetrahydrofuran and is stable only at 77 K. Five-coordinate rhodium(II) porphyrins with bound NO and O_2 ligands have been reported in the literature, but these species are often described as containing a rhodium(III) ion.[15]

In this paper, we report the electrochemical properties and spectral characterization of bis(dimethylamine)(tetraphenylporphinato)rhodium(III) chloride, (TPP)Rh(NH(CH$_3$)$_2$)$_2^+$Cl$^-$, and (dimethylamine)(chlorotetraphenylporphinato)rhodium(III), (TPP)Rh(NH(CH$_3$)$_2$)Cl. These complexes will be abbreviated as (TPP)Rh(L)$_2^+$Cl$^-$, and (TPP)Rh(L)Cl where L = dimethylamine.

Experimental Section

Instrumentation and Methods. IR spectra were measured on a Perkin-Elmer 1330 infrared spectrophotometer. UV-visible spectra were recorded on a Hitachi 110 spectrophotometer or a Tracor Northern 1710 holographic optical spectrometer/multichannel analyzer. NMR spectra were taken on a Varian FT-80 spectrometer. ESR spectra were recorded on an IBM Model ED-100 electron spin resonance system. A YSI Model 31 conductivity bridge was used to perform conductivity measurements. Cyclic voltammetric and polarographic measurements were obtained by using an EG&G Princeton Applied Research Model 174A/175 polarographic analyzer/potentiostat coupled with an EG&G Model 9002A X-Y recorder for potential scan rates less than 500 mV/s or a Tektronix 5111 storage oscilloscope for scan rates equal to or larger than 500 mV/s. The working and counter electrodes used were platinum, except in the case of the thin-layer spectroelectrochemical cell, where a gold-minigrid electrode was used. Potentials were all measured vs. a saturated calomel electrode (SCE), which was separated from the bulk of the solution by means of a fritted-glass-disk junction. Potential measurements were also made vs. the ferrocene/ferrocenium (Fc/Fc$^+$) couple for the purpose of evaluating liquid-junction-potential differences between different solvents. Low-temperature experiments were performed by cooling the cell with a dry ice/acetone bath to a constant temperature, monitored by a thermocouple. Bulk controlled-potential coulometry was carried out on an EG&G Princeton Applied Research Model 174 potentiostat/Model 179 coulometer system, coupled with a Shimadgu R-12 laboratory recorder. Thin-layer spectroelectrochemical measurements were made wth an IBM 225/2A voltammetric analyzer coupled with a Tracor Northern 1710 spectrometer/multichannel analyzer.

Materials. $RhCl_3 \cdot 3H_2O$ was purchased from Matthey Bishop, Inc., Malvern, PA. All solvents used in the synthesis of the rhodium porphyrins were either reagent or chemical grade. For the electrochemical and spectroscopic measurements, spectroscopic grade pyridine (py) was distilled over KOH. Reagent grade benzonitrile (PhCN) was vacuum-distilled over P_2O_5 before use. Spectroscopic grade THF was used without further purification. Tetra-*n*-butylammonium perchlorate (TBAP) was purchased from Eastman Kodak Co., twice recrystallized from ethyl alcohol, and stored in a vacuum oven at 40 °C. Unless otherwise noted, 0.1 M TBAP was used as a supporting electrolyte for the cyclic voltammetric measurements while 0.5 M TBAP was used for bulk solution electrolysis and 0.2 M TBAP was used for the spectroelectrochemical measurements.

Syntheses of the rhodium complexes were performed by literature

† Present Address: L'Air Liquide CRCD, 78350 Jouy-en-Josas, France.

(1) Fleischer, E. B.; Sadasivan, N. *J. Chem. Soc., Chem. Commun.* **1967**, 159.
(2) Sadasivan, N.; Fleischer, E. B. *J. Inorg. Nucl. Chem.* **1968**, *30*, 591.
(3) Fleischer, E. B.; Thorp, R.; Venrable, D. *J. Chem. Soc., Chem. Commun.* **1969**, 475.
(4) Fleischer, E. B; Lavallee, D. *J. Am. Chem. Soc.* **1967**, *89*, 7132.
(5) Fleischer, E. B.; Dixon, F. L.; Florian, R. *Inorg. Nucl. Chem. Lett.* **1973**, *9*, 1303.
(6) Cohen, I. A.; Chow, B. C. *Inorg. Chem.* **1974**, *13*, 488.
(7) Yoshida, Z.; Ogoshi, H.; Omura, T.; Watanabe, E.; Kurosaki, T. *Tetradhedron Lett.* **1972**, *11*, 1077.
(8) Ogoshi, H.; Setsune, J.; Omura, T.; Yoshida, Z. *J. Am. Chem. Soc.* **1975**, *97*, 6461.
(9) James, B. R.; Stynes, C. V. *J. Chem. Soc., Chem. Commun.* **1972**, 1261.
(10) Wayland, B. B.; Newman, A. R. *J. Am. Chem. Soc.* **1979**, *101*, 6472.
(11) Wayland, B. B.; Woods, B. A.; Pierce, R. *J. Am. Chem. Soc.* **1982**, *104*, 302.
(12) Wayland, B. B.; Duttahmed, A.; Woods, B. A. *J. Chem. Soc., Chem. Commun.* **1983**, 142.
(13) Ogoshi, H.; Setsune, J.; Yoshida, Z. *J. Am. Chem. Soc.* **1977**, *99*, 3869.
(14) James, B. R.; Stynes, C. V. *J. Am. Chem. Soc.* **1972**, *94*, 6225.
(15) Wayland, B. B.; Newman, A. R. *Inorg. Chem.* **1981**, *20*, 3093.
(16) Hoshino, M.; Yasufuku, K.; Konishi, S.; Imamura, M. *Inorg. Chem.* **1984**, *23*, 1982.
(17) Yamamoto, S.; Hoshino, M.; Yasufuku, K.; Imamura, M. *Inorg. Chem.* **1984**, *23*, 195.
(18) Barnes, C. E. Dissertation Thesis, Stanford University, 1982.

0020-1669/85/1324-4515$01.50/0

Table I. Spectral Data of Complexes Electrogenerated at Room Temperature

compd	solvent	electrode reacn	λ_{max} ($\epsilon \times 10^{-3}$), nm (M^{-1} cm^{-1})			
$(TPP)Rh(L)_2^+Cl^-$	PhCN	none	421 (272)	530 (25.0)	564 (58)	
		1st redn	406 (206)	497 (15.6)		
		2nd redn	836 (19.4)			
		1st oxidn	408 (90.7)	590 (12.1)	637 (13.7)	754 (3.8)
		2nd oxidn	418 (54.1)	664 (19.0)		
	py	none	422 (242)	530 (26.8)	565 (5.6)	
		1st redn	407 (186)	496 (16.0)		
		2nd redn	407 (63.9)	456 (53.0)		
(TPP)Rh(L)Cl	PhCN	none	426 (234)	536 (25.4)	570 (7.6)	
		1st redn	406 (184)	497 (14.0)		
		2nd redn	835 (15.2)			
		1st oxidn	412 (103)	582 (14.1)	645 (12.8)	730 (13.3)
		2nd oxidn	421 (58.7)	622 (22.0)		
	py	none	424 (23.1)	536 (25.5)	571 (5.9)	
		1st redn	407 (179)	498 (20.0)		
		2nd redn	407 (51.2)	456 (54.3)		

methods[5] and produced a mixture of mono- and bis(dimethylamine)-(tetraphenylporphinato)rhodium(III). (Earlier reports refer only to the bis adduct of rhodium(III) porphyrins.) A typical experiment is described as follows: $RhCl_3 \cdot 3H_2O$ (850 mg, 3.23 mmol) was refluxed in 50 mL of dimethylformamide (DMF) for 30 min. A suspension of H_2TPP (500 mg, 0.81 mmol) in DMF (500 mL) was then added to the solution and the mixture allowed to reflux for 24 h. After being cooled down to room temperature the reaction mixture was poured over 500 mL of water and extracted by CH_2Cl_2. The obtained solution was concentrated to a small volume and passed through an activated alumina column. Elution with CH_2Cl_2 as solvent gave a first fraction of unreacted H_2TPP followed by a second one characterized as (TPP)Rh(L)Cl. The bis adduct, $(TPP)Rh(L)_2^+Cl^-$ was eluted by using a 100:1 mixture of CH_2Cl_2/CH_2OH. Further purification was achieved by recrystallization of (TPP)Rh(L)Cl in CH_2Cl_2/*n*-hexane or $(TPP)Rh(L)_2^+Cl^-$ in CH_2Cl_2/CH_3OH/*n*-hexane. These two complexes were studied spectroscopically and showed the following characteristics. $(TPP)Rh(HN(CH_3)_2)Cl$: UV–visible spectra, see Table I; IR (CsI pellet, cm^{-1}) 345 (ν_{Rh-Cl}), 890 and 1310 ($\nu_{Rh-N(amine)}$) plus usual porphyrin bands; ^1H NMR ($CDCl_3$, δ) 8.88 (py H, s, 8 H), 7.75 (phenyl H, m, 12 H), −3.27 (amine CH_3, s, 6 H), −5.43 (amine NH, br, 1 H); molar conductivity (CH_2Cl_2) ~0.0 Ω^{-1} mol^{-1} cm^2.

$(TPP)Rh(HN(CH_3)_2)_2^+Cl^-$: UV–visible spectra, see Table I; IR (CsI pellet, cm^{-1}) 890 and 1310 ($\nu_{Rh-N(amine)}$) plus usual porphyrin bands (it is noted that this complex does not show any stretching frequency at 345 cm^{-1}); ^1H NMR ($CDCl_3$, δ) 8.97 (py H, s, 8 H), 7.79 (phenyl H, m, 12 H), −3.40 (amine CH_3 s, 12 H), −4.20 (amine NH, br, 2 H); molar conductivity (CH_2Cl_2) 3.9×10^3 Ω^{-1} mol^{-1} cm^2.

Results and Discussion

Room-Temperature Reduction of (TPP)Rh(L)Cl and (TPP)Rh(L)$_2^+$Cl$^-$ in Benzonitrile and THF. Cyclic voltammograms of (TPP)Rh(L)Cl and $(TPP)Rh(L)_2^+Cl^-$ are similar in PhCN, 0.1 M TBAP, and an example is shown in Figure 1. At room temperature, (TPP)Rh(L)Cl undergoes three reversible and one irreversible electron-transfer processes between +1.90 and −2.00 V vs. SCE (Figure 1a). The bis(dimethylamine) complex also undergoes four electron-transfer reactions in this potential range (Figure 1b), but at all scan rates, only two of the processes are reversible (reactions 2 and 3).

The first reduction of both (TPP)Rh(L)Cl and $(TPP)Rh(L)_2^+Cl^-$ is irreversible in the sense that there are no coupled reoxidation peaks for these two processes. These reductions are labeled as peak 1 in Figure 1. The shape and height of the current voltage curves for peak 1 are similar for both Rh(III) complexes and indicate a fast chemical reaction following a rapid (diffusion-controlled) single-electron transfer. The peak currents for the first reduction are approximately equal to those for the reversible one-electron oxidation of the same complex, suggesting a one-electron transfer for the initial electroreduction step. For both complexes, $E_p - E_{p/2} = 60$ ● 10 mV and $i_p/v^{1/2}$ is constant, confirming an initial diffusion-controlled one-electron reduction.

A small oxidation peak is located between $E_p = -0.20$ and −0.30 V for both compounds but is not present when the cathodic potential scan is terminated before the first reduction peak. The exact potential of the oxidation peak (labeled peak 1′) varies with scan rate as demonstrated in Figure 2. The direction and

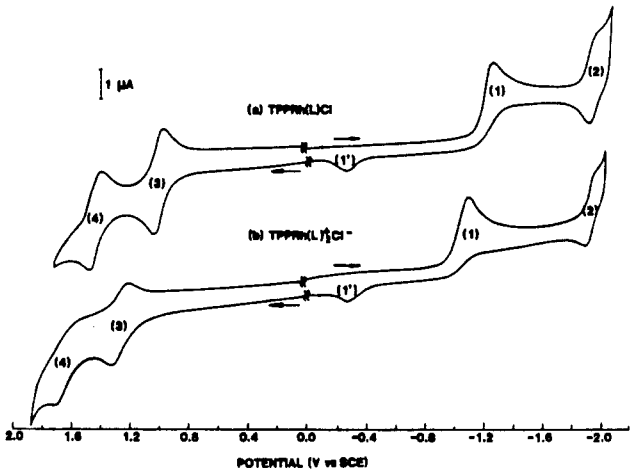

Figure 1. Cyclic voltammograms of (a) 4.2×10^{-4} M (TPP)Rh(L)Cl and (b) 4.8×10^{-4} M $(TPP)Rh(L)_2^+Cl^-$ in PhCN, 0.1 M TBAP (scan rate 0.1 V/s).

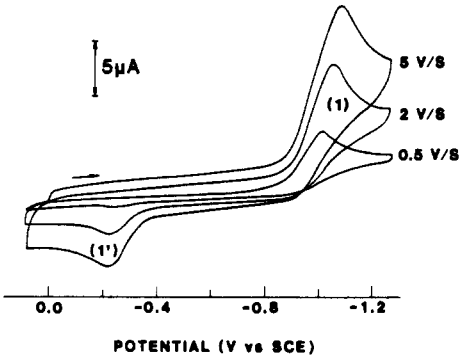

Figure 2. Cyclic voltammograms illustrating the first reduction and the reoxidation of $(TPP)Rh(L)_2^+Cl^-$ at various scan rates in PhCN, 0.1 M TBAP.

magnitude of the potential shift is consistent with the lack of a cathodic peak coupled directly to peak 1′ and the EC nature of the oxidation process.

Controlled-potential electrolysis was carried out in bulk and thin-layer cells, and the products of each reduction were monitored by electronic absorption spectra and ESR measurements. In both cases, 1.0 ± 0.1 electron was required to complete the first reduction. The molar absorptivities and spectral band maxima of the singly reduced $(TPP)Rh(L)_2^+Cl^-$ in PhCN are given in Table I. Upon electroreduction the Soret band decreases in intensity and shifts from 421 to 406 nm, the visible bands at 530 and 564 nm disappear, and a new peak appears at 497 nm. This is shown in Figure 3a. A similar spectrum is observed for singly reduced (TPP)Rh(L)Cl, which has peak maxima at 406 and 497 nm. No additional absorption peaks are observed between 600 and 900

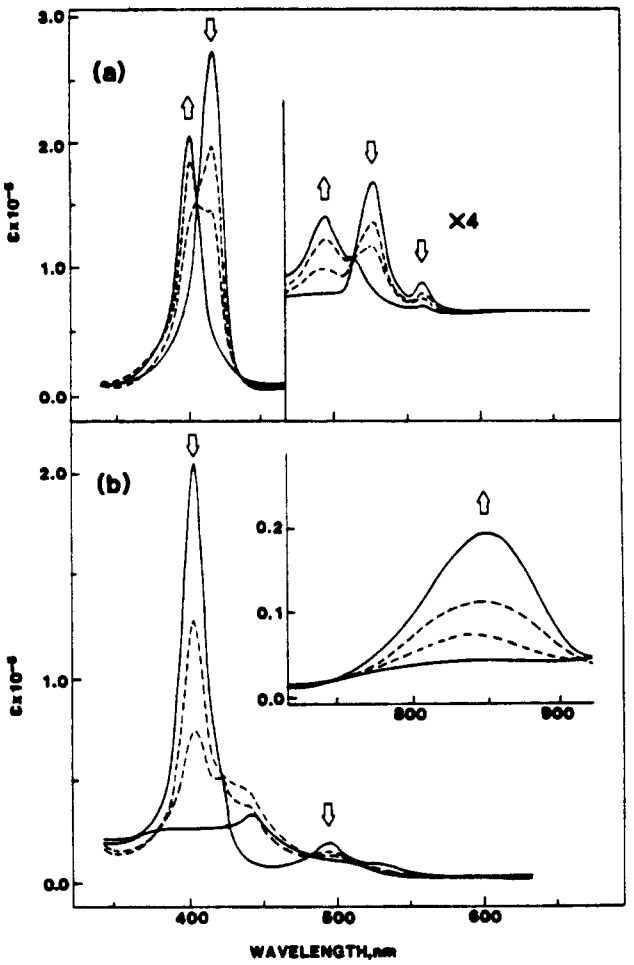

Figure 3. Electronic absorption spectra of (a) singly reduced and (b) doubly reduced (TPP)Rh(L)$_2^+$Cl$^-$ in PhCN, 0.2 M TBAP.

nm, thus strongly suggesting the absence of a porphyrin ring centered reduction (which would correspond to anion radical formation). The small changes in the Soret peak intensity and the lack of strong aborption bands above 550 nm suggest electrode reactions in which electron addition occurs at the central metal.[19] For the specific case of the investigated compounds, the reaction corresponds to generation of a Rh(II) species from the initial Rh(III) complexes.

Electronic absorption spectra of the reduced Rh(III) porphyrins in PhCN are different from those of four-coordinate (TPP)Rh^{II},[16] or five-coordinate (TPP)Rh(O_2).[14,15] The electronic absorption spectrum of [(TPP)Rh]$_2$ is reported to have a Soret band at 415 nm and a Q band at 526 nm.[16,17] However, the dimer was never isolated from the flash photolysis mixture, and its assignment was tentative.[17] The absorption spectrum reported for [(TPP)Rh]$_2$ is nearly identical with that of (TTP)Rh(H), which has a Soret band at 416 nm, a Q band at 522 nm, and an additional weak band at 600 nm.[18] The shape of the spectra presented in Figure 3 resembles that of both the reported Rh(II) dimer and hydride but differs in the location of the Q band, which is shifted by about 30 nm (to 497 nm), and the Soret band, which is shifted by 9 nm. The similarity of the spectra for the Rh(II) dimer and hydride to the spectrum of our Rh(II) compound suggests that our compound is of a similar nature.

Axial ligation could account for the difference in the electronic absorption spectra between this work and that in the literature. An alternative explanation is that [(TPP)Rh]$_2$ is formed in this work but the absorption spectrum reported in the literature[16,17] for the dimer was actually for (TPP)Rh(H). At the present, we are inclined to believe the latter case is true. The postulate of

(19) Kadish, K. M.; Davis, D. G.; Fuhrhop, J.-H. *Angew. Chem.* **1972**, *11*, 1014.

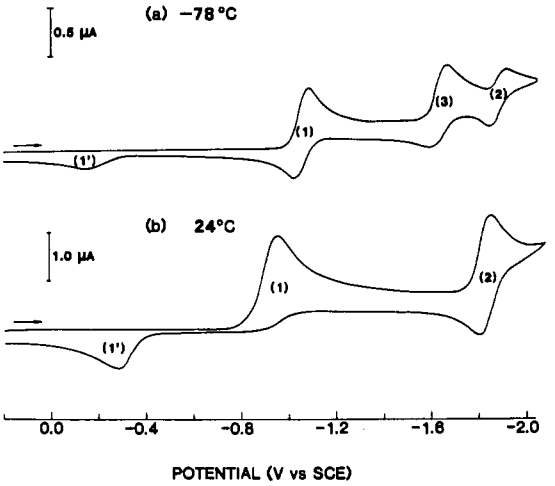

Figure 4. Cyclic voltammogram of (TPP)Rh(L)$_2^+$Cl$^-$ in THF, 0.2 M TBAP at (a) −78 °C and (b) 24 °C (scan rate 0.2 V/s).

a Rh(II) dimer formation upon the one-electron reduction of the Rh(III) complex is strengthened by the fact that the reduction product is diamagnetic, as evidenced by the lack of an ESR signal. The reaction of O_2 with rhodium(II) porphyrin dimers is known to produce an oxygen adduct.[15] In this study, when oxygen (air) was added to a solution of the first reduction product, (TPP)Rh(O_2) was formed and easily detected by its characteristic ESR signal.

Identical electronic absorption spectra were obtained after the second reduction of both Rh(III) complexes and are illustrated in Figure 3b for reduced (TPP)Rh(L)$_2^+$Cl$^-$. During reduction the Soret band decreased in intensity as did the peak at 534 nm. At the same time, a new peak appeared at 836 nm. The position and the shape of the absorbance at 836 nm indicates formation of an anion radical. The second reduction of (TPP)Rh(L)Cl and (TPP)Rh(L)$_2^+$Cl$^-$ (peak 2, Figure 1) is reversible in PhCN, 0.1 M TBAP, and occurs at −1.96 V for both compounds. The peak separation is 35 ± 5 mV, indicating two electrons transferred. Current integration of the second reduction gives one electron transferred per rhodium metal, thus implying a dimeric unit. The product of the second reduction is diamagnetic, which also agrees with a two-electron transfer.

Low-Temperature Experiments. The electrochemistry of (TPP)Rh(L)$_2^+$Cl$^-$ at low temperatures is different than at room temperature. This effect of temperature is presented in Figure 4, which illustrates the reduction of (TPP)Rh(L)$_2^+$Cl$^-$ in THF at −78 °C. At this temperature, the first reduction wave is reversible and occurs at $E_{1/2}$ = −1.05 V. A value of $E_p - E_{p/2}$ = 60 ± 5 mV is obtained for the cathodic peak. In addition, the peak separation, $E_{pa} - E_{pc}$ = 60 ± 5 mV, and $i_p/v^{1/2}$ is constant. A second reversible one-electron diffusion-controlled reduction occurs at −1.63 V. This wave has a peak separation of 60 ± 5 mV, $E_p - E_{p/2}$ = 60 ± 5 mV, and an $i_p/v^{1/2}$ value that is constant. This wave is coupled with a decrease in the current for the wave at −1.87 V. These changes at low temperature are not seen for (TPP)Rh(L)Cl.

The temperature effect is clearly the result of slowing down the chemical reaction following the first reduction of (TPP)Rh(L)$_2^+$Cl$^-$. At room temperature, the chemical reaction is too fast for any intermediates to be seen. However, at reduced temperatures detection of an intermediate on the electrochemical time scale is possible. No ESR signal was observed when the first reduction was carried out at low temperatures, indicating the one electron reduction product reacts faster than the time required to freeze the solution. The chemical reaction that follows the first reduction of (TPP)Rh(L)Cl must be much faster than that for (TPP)Rh(L)$_2^+$Cl$^-$ since low temperature does not alter the current–voltage curves.

Reaction Mechanism. Analysis of the electrochemical data coupled with the electronic absorption spectra, ESR spectra, and low-temperature electrochemistry suggests the mechanism shown

Table II. Half-Wave Potentials and Peak Potentials (V vs. SCE) for Oxidation and Reduction of the Rhodium Complexes

			oxidn		redn		
compd	solvent	temp, °C	peak 2	peak 3	peak 1′	peak 1	peak 2
$(TPP)Rh(L)_2^+Cl^-$	PhCN	24	1.70[a]	1.27	−0.24[a]	−1.06[b]	−1.95
	py	24			−0.40[a]	−0.99[b]	−1.90
	THF	24			−0.22[a]	−0.96[b]	−1.83
		−78			−0.15[a]	−1.07[b]	−1.87
						−1.05[d,e]	−1.63[d,e]
(TPP)Rh(L)Cl	PhCN	24	1.43	1.00	−0.24[a]	−1.28[b]	−1.96
						−1.03[b,c]	
	py	24			−0.40[a]	−1.24[b]	−1.90
						−0.99[b,c]	
	THF	24			−0.22[a]	−1.18[b]	−1.84
						−0.96[b,c]	
		−78			−0.14[a]	−1.31[b]	−1.87

[a] Anodic peak potential, E_{pa}. This peak was only observed after scanning negatively past the first reduction (peak 1). [b] Cathodic peak potential, E_{pc}. [c] E_{pc} cathodic peak potential of second sweep. [d] Found only at low temperature (see Figure 4). [e] Represents $E_{1/2}$ for low-temperature wave.

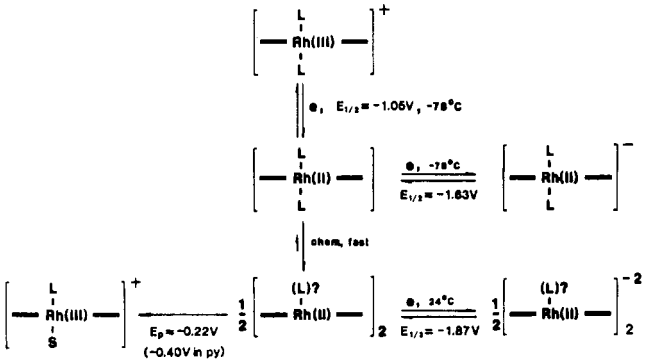

Figure 5. Reduction mechanism for $(TPP)Rh(L)_2^+Cl^-$ and (TPP)Rh(L)Cl.

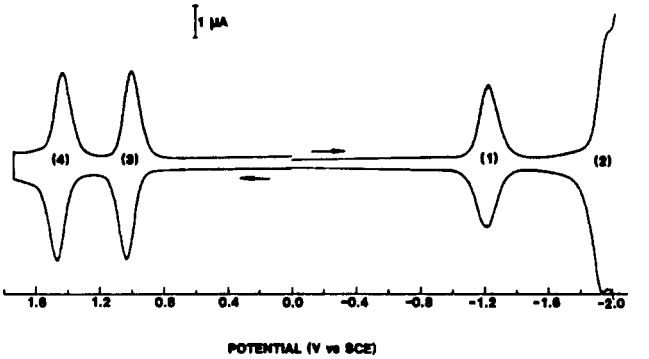

Figure 6. Cyclic differential pulse voltammograms of (TPP)Rh(L)Cl in PhCN, 0.1 M TBAP (scan rate 0.002 V/s).

in Figure 5 for reduction of $(TPP)Rh(L)_2^+Cl^-$. A similar dimerization occurs after reduction of (TPP)Rh(L)Cl, but in this case no new peaks are observed at low temperature, thus suggesting a very rapid dimerization.

Both Rh(III) complexes are reduced by a single electron transfer step to yield a transient six-coordinate Rh(II) species in PhCN. This species (which for $(TPP)Rh(L)_2^+Cl^-$ can be detected at low temperatures on the electrochemical time scale) rapidly reacts to form the proposed Rh(II) dimer, which is reduced by a two-electron-transfer process at approximately −1.9 V (see Table II).

Reoxidation of the proposed dimer produces the same Rh(III) species for both (TPP)Rh(L)Cl and $(TPP)Rh(L)_2^+Cl^-$. This is evidenced by identical electronic absorption spectra after a single reduction–reoxidation cycle and the same peak at ~−1.9 V. The electronic absorption spectrum of the electrochemically generated Rh(III) species is sensitive to different solvents and is represented in Figure 5 as (TPP)Rh(L)S, where S is a solvent molecule. This species is clearly detected electrochemically by the appearance of a new wave at $E_p = -1.03$ V on the second reduction cycle of (TPP)Rh(L)Cl in PhCN. $(TPP)Rh(L)_2^+Cl^-$ is already reduced at $E_p = -1.06$ V on the first negative scan in PhCN, and a new reduction wave is not observed on the second cycle.

Additional evidence for the mechanism shown in Figure 5 comes from cyclic differential-pulse voltammograms carried out in PhCN, 0.1 M TBAP. This method was previously used to evaluate the overall reduction mechanism of (TPP)CrCl(L) in CH_2Cl_2, 0.1 M TBAP, media[20] and for the present case gives almost identical current–voltage curves as have been reported for Cr(III) reduction, as shown in Figure 6. As seen in this figure, well-defined, coupled oxidation–reduction peaks are observed for three of the four processes. The presence of an oxidation peak coupled to the first reduction indicates some dissociation of the proposed Rh(II) dimer occurs prior to reoxidation. The driving force for the dissociation

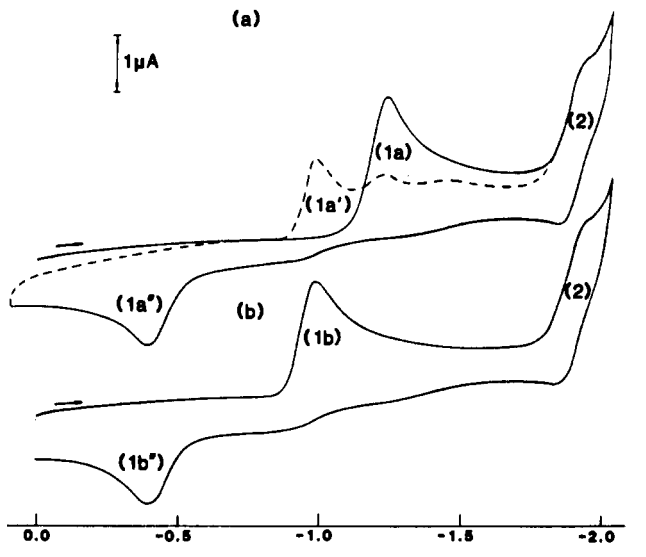

Figure 7. Cyclic voltammograms of (a) 1.01×10^{-3} (TPP)Rh(L)Cl and (b) 1.06×10^{-3} M $(TPP)Rh(L)_2^+Cl^-$ in pyridine, 0.1 M TBAP: (—) first scan; (- -) second scan (scan rate = 0.1 V/s).

is the greater than 800-mV difference between potentials for oxidation of a monomeric Rh(II) species (at $E_p \approx -1.0$ V) and oxidation of the proposed dimer (at $E_p \approx -0.2$ V).

Reduction of $(TPP)Rh(L)_2^+Cl^-$ and (TPP)Rh(L)Cl in Pyridine. Reduction of the Rh(III) complexes in pyridine gives current–voltage curves that are qualitatively and quantitatively similar to those observed in PhCN. At all scan rates up to 10 V/s both compounds undergo an irreversible first reduction and a reversible second reduction. This is illustrated in Figure 7, and potentials for all of the peaks in three solvents are given in Table II. Only the reductions are presented in pyridine since oxidations of the

(20) (a) Bottomley, L. A.; Kadish, K. M. *J. Chem. Soc., Chem. Commun.* **1981**, 112. (b) Bottomley, L. A.; Kadish, K. M. *Inorg. Chem.* **1983**, *22*, 342.

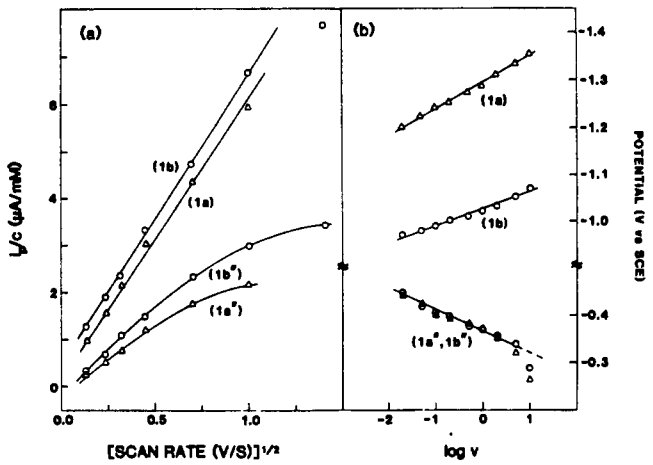

Figure 8. Plots of (a) i_p/C (where C = porphyrin concentration) vs. $v^{1/2}$ and (b) E_p vs. log v for the reduction and reoxidation of (TPP)Rh(L)$_2^+$Cl$^-$ and (TPP)Rh(L)Cl in neat pyridine. Peaks are identified in Figure 7.

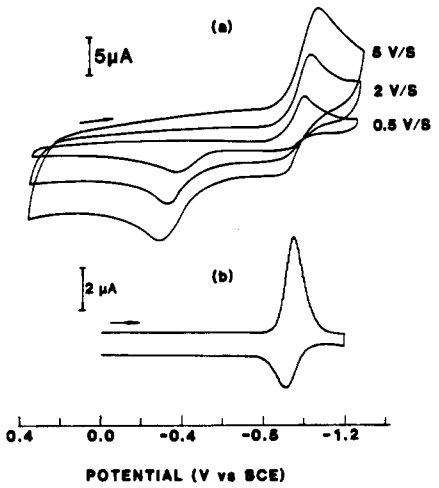

Figure 9. (a) Cyclic voltammograms for the first reduction of 1.06×10^{-3} M (TPP)Rh(L)$_2^+$Cl$^-$ at various scan rates in pyridine, 0.1 M TBAP. (b) Cyclic differential-pulse voltammograms of the same compound at 0.002 V/s.

Rh(III) complexes occur beyond the anodic potential limit of the solvent.

The initial one-electron reduction of (TPP)Rh(L)Cl in neat pyridine occurs at $E_{pc} = -1.24$ V at a scan rate of 100 mV/s (peak 1a, Figure 7). This is very close to the peak potential for reduction of the same complex in PhCN (see Table II). When corrected for liquid potential, the actual potential difference between the two solvents is only 30 mV. The current–voltage curves are well-defined in pyridine and have a shape indicative of a diffusion-controlled one-electron transfer ($|E_p - E_{p/2}| = 60 \pm 5$ mV). In addition, $i_p/v^{1/2}$ is constant, as shown in Figure 8, again indicating diffusion-controlled process.

Reversal of the scan direction at potentials more negative than −1.27 V shows the presence of a well-defined oxidation process at $E_p \cong -0.40$ V (Figure 9). This is negatively shifted by 160 mV from the value of $E_{pa} = -0.24$ V in PhCN (see Table II) where a Rh(II) dimer is postulated to be the reactant. The potential of this peak shifts anodically with increase in scan rate and has a maximum current that increases with scan rate as shown in Figure 8a. It is not proportional to the square root of the scan rate. This oxidation peak is identical for both compounds and does not appear until cathodic scans have swept beyond the first reduction peak (peak 1a or peak 1b in Figure 7), clearly indicating that the reacting species for the oxidation is generated as a product of the first reduction.

The oxidation peak at ≅ −0.4 V for (TPP)Rh(L)Cl (Peak 1a″, Figure 7) is observed on the first, second, and all subsequent

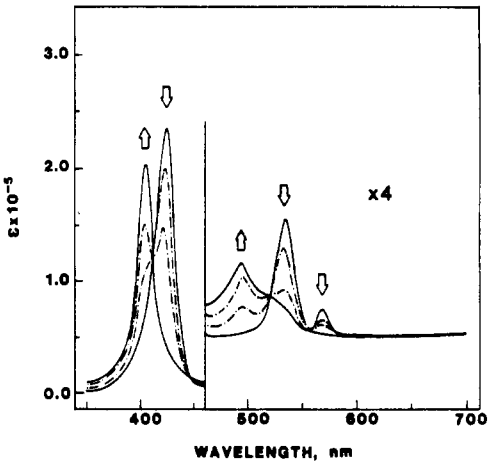

Figure 10. Electronic absorption spectra of the neutral and the singly reduced (TPP)Rh(L)Cl in neat pyridine, 0.2 M TBAP. Spectra were obtained during controlled-potential reduction at −1.35 V.

potential sweeps. This is not the case for the first reduction process where the second and all subsequent scans give a new, well-defined, reduction peak, which is shifted from $E_{pc} = -1.24$ V to $E_{pc} = -0.99$ V. This is illustrated in Figure 7a and supports the formation of [(TPP)Rh(L)(py)]$^+$ as the reoxidation product. A similar irreversible displacement of Cl$^-$ by pyridine is observed for the reduction and reoxidation of (TPP)CrCl in pyridine,[20] and similar current–voltage curves are obtained.

It is significant that cyclic voltammograms for the reduction and reoxidation of (TPP)Rh(L)$_2^+$Cl$^-$ in pyridine are identical with those obtained for reduction of (TPP)Rh(L)Cl on the second and all subsequent scans. This is shown in Figure 7b. An irreversible but diffusion-controlled reduction peak for (TPP)Rh(L)$_2^+$Cl$^-$ is observed at $E_{pc} = -0.99$ V (at 100 mV/s). Cyclic voltammograms obtained as a function of scan rate and a cyclic differential pulse voltammogram (at 0.005 V/s) for the reduction of (TPP)Rh(L)$_2^+$Cl$^-$ in neat pyridine are shown in Figure 9. Similar to the reduction carried out in PhCN, no reverse peak is obtained by cyclic voltammetry, although with cyclic differential pulse voltammetry a coupled reduction–oxidation process at ≃ −1.0 V is indicated.

The above results suggest that, in pyridine, the reactant is (TPP)Rh(L)Cl or (TPP)Rh(L)$_2^+$ on the first scan but that on all subsequent scans [(TPP)Rh(L)(py)]$^+$ or [(TPP)Rh(py)$_2$]$^+$ is reduced at the electrode surface. Displacement of an amine or chloride ion by pyridine does not occur before reduction. This is demonstrated by the similar electronic absorption spectra of the unreduced complexes in PhCN and neat pyridine as well as by an NMR study of the complexes in $CDCl_3$ and deuterated pyridine. This latter study shows that identical NMR spectra are obtained in both solvents, confirming that neither chloride ion nor $NH(CH_3)_2$ is displaced by pyridine as an axial ligand.

The cathodic peak potential for the first reduction varies little upon addition of pyridine to PhCN solutions. On the other hand, the reoxidation peak of Rh(II) at ≈ −0.24 V in neat PhCN shifted to a more negative potential as the concentration of pyridine increased. A plot of E_{pa} vs. log C_{py} has a slope of 30 ± 5 mV. This shift of the reoxidation peak is due to two factors. The first is the thermodynamic stabilization of the Rh(III) complex by pyridine. The second is the dependence of the peak potential on the rate constant(s) of the coupled chemical reaction(s), which are dependent on the concentration of pyridine in solution.

Figure 10 shows electronic absorption spectra obtained during controlled-potential reduction of (TPP)Rh(L)Cl in neat pyridine. Upon reduction in pyridine, changes occur in both the Soret region, where λ_{max} shifts from 424 to 407 nm, and in the visible region of the spectrum, where the peaks at 536 and 571 nm decrease and a new peak at 498 nm appears. Similar spectral changes were observed for reduced (TPP)Rh(L)$_2^+$Cl$^-$, and for both compounds, well-defined isobestic points were obtained, indicating the absence of chemical intermediates in any appreciable concentration.

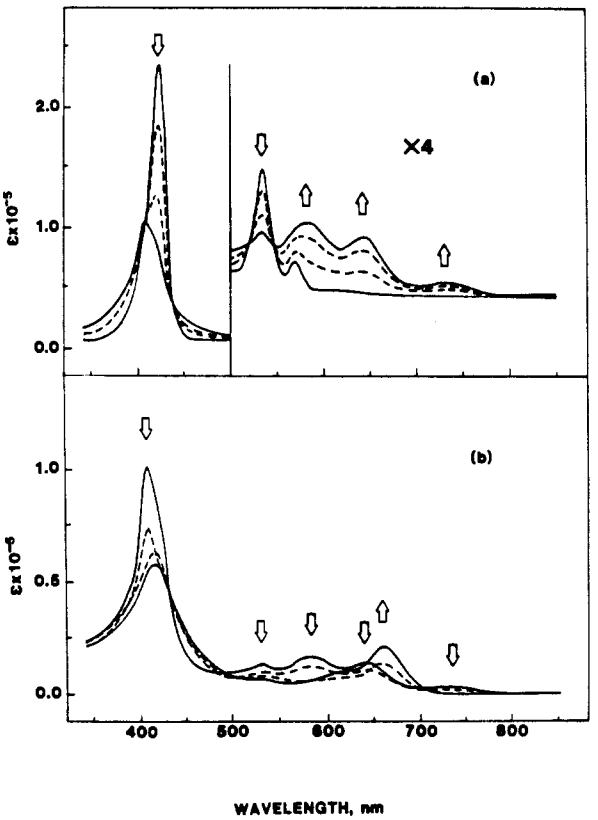

Figure 11. Electronic absorption spectra taken at an optically transparent thin-layer electrode of (a) neutral and singly oxidized $(TPP)Rh(L)_2^+Cl^-$ in PhCN, 0.2 M TBAP, and (b) singly and doubly oxidized $(TPP)Rh(L)_2^+Cl^-$ in PhCN, 0.2 M TBAP.

Spectral wavelengths and molar absorptivities of each electrogenerated species are listed in Table I. As seen in this table, the Rh(II) complexes have similar spectra in PhCN and py.

Oxidations of Rh(III) Complexes. The first and second oxidations of (TPP)Rh(L)Cl occur at +1.00 and +1.43 V in PhCN and correspond to the stepwise formation of the cation radical and dication. The first oxidation peak (peak 3, Figure 1) has an identical half-wave potential as that reported for the oxidation of (TPP)RhCl in CH_2Cl_2, while the second oxidation (peak 4, Figure 1) has been shifted by 80 mV from that for the second oxidation of (TPP)RhCl ($E_{1/2}$ = 1.35 V)[15] (see Table II). Two oxidations are also observed for $(TPP)Rh(L)_2^+Cl^-$, but at all scan rates, only the first reaction is reversible. This is shown in Figure 1b at a scan rate of 100 mV/s. Both oxidation potentials are shifted anodically from values observed for (TPP)RhCl and occur at $E_{1/2}$ = 1.27 V and E_{pa} = 1.70 (at 100 mV/s), respectively.

Thin-layer spectra were taken during the first and second oxidation of $(TPP)Rh(L)_2^+Cl^-$ and (TPP)Rh(L)Cl. These spectra are illustrated in Figure 11 for $(TPP)Rh(L)_2^+Cl^-$. The one-electron oxidation generates a spectrum with a decreased Soret band intensity at 408 nm and several new broad bands at 590, 637, and 754 nm. In addition, isobestic points are located at 432, 514, and 544 nm, strongly suggesting the presence of only two species in solution.

The final thin-layer spectrum of first oxidized species clearly indicates the presence of a Rh(III) cation radical. This assignment is confirmed by the ESR spectrum of the species generated after bulk coulometric abstraction of 1.0 ± 0.1 electron at 1.40 V. This radical-like spectrum has a single absorbance at g = 2.003 and agrees well with values of g = 2.001 for other porphyrin cation radicals of Rh(III).[15]

Similar ESR and electronic absorption spectra were observed for the singly oxidized (TPP)Rh(L)Cl complex in PhCN. Controlled-potential electrolysis at 1.20 V led to the abstraction of 1.0 electron and gave a cation radical-like species with absorbances at 412, 582, 645, and 730 nm in PhCN. ESR spectra of frozen PhCN/0.5 M TBAP solutions showed a signal at g = 2.000, also indicating cation radical formation. Finally, application of a controlled potential of 0.0 V to the singly oxidized species led to the disappearance of ESR signal and the quantitative reappearance of the original electronic absorption spectrum. This was true for both $(TPP)Rh(L)_2^+Cl^-$ and (TPP)Rh(L)Cl.

Acknowledgment. The support of the National Science Foundation (Grant No. 8215507) is gratefully acknowledged.

Registry No. (TPP)Rh(L)Cl, 99147-88-3; $[(TPP)Rh(L)Cl]^+$, 99129-05-2; $[(TPP)Rh(L)Cl]^{2+}$, 99129-06-3; $(TPP)Rh(L)_2^+Cl^-$, 51669-90-0; $[(TPP)Rh(L)_2^+Cl^-]^+$, 99129-09-6; $[(TPP)Rh(L)_2^+Cl^-]^{2+}$, 99129-10-9; $[(TPP)Rh(L)_2^+Cl^-]^-$, 99129-07-4; $[(TPP)Rh(L)Cl]^-$, 99129-08-5.